ARTICLES

Phase-shift analysis of *NN* scattering below 160 MeV: Indication for a strong tensor force

R. Henneck
Paul-Scherrer-Institut, CH-5232 Villigen, Switzerland
(Received 13 April 1992)

A new phase-shift analysis of *NN* scattering in the energy range 15–160 MeV is presented. The analysis is based on the carefully reviewed world *pp* + *np* data, including recent results for higher-order spin observables in *n-p* scattering. The latter are essential to determine the mixing parameter ε_1 which is directly related to the isoscalar tensor force. ε_1 displays a high trend, in agreement with recent analyses above 140 MeV, and is only reproduced by potential models with a strong tensor force. The prediction of the full Bonn potential is too low by 20% for energies above 40 MeV. All other $I=0$ phase shifts show agreement with potential models; in particular, the notorious problem with $^1P_1$ around 50 MeV has disappeared. Around 25 MeV a ten parameter fit based purely on *np* data agrees with the corresponding fit to the *pp* data and reveals no indication of anomalous charge independence breaking.

PACS number(s): 21.30.+y, 13.75.Cs, 21.45.+v, 25.10.+s

I. INTRODUCTION

Of all contributions to the fundamental nucleon-nucleon (*NN*) interaction, the tensor force represents one of the most important and most interesting components. This force has the unique characteristic of mixing states with different angular momenta $L_\pm = J \pm 1$, where J is the total angular momentum. Its subtle, nevertheless characteristic manifestations for the deuteron properties were recognized as such from very early on: The nonvanishing quadrupole moment and the anomalous magnetic moment (i.e., the fact that the magnetic moment is slightly different from the sum of the neutron and proton magnetic moments) were taken by Schwinger [1] as evidence for a tensor component. Bethe [2] recognized the dominant contribution of the tensor force to the binding energy of the deuteron. The latter finding touches upon a problem still virulent today: the question of whether nuclear binding energies can quantitatively be understood in terms of two-nucleon ($2N$) forces. Exact calculations of the ^{3}H binding energy B_t show that without three-body ($3N$) forces the measured binding energy can only be reproduced for a weak tensor force [3–5]. The calculated binding energy depends strongly on the tensor contributions of the *NN* potentials, which can be characterized by the deuteron D state probability P_D [3]:

$$B_t(\text{Bonn } A,\ P_D = 4.4\%) = -8.32 \text{ MeV},$$

$$B_t(\text{Bonn } B,\ P_D = 5.0\%) = -8.13 \text{ MeV},$$

$$B_t(\text{Bonn } C,\ P_D = 5.6\%) = -7.99 \text{ MeV},$$

$$B_t(\text{Paris},\ P_D = 5.8\%) = -7.46 \text{ MeV}.$$

Although there is some debate about the influence of other partial waves, e.g., $^1S_0$ and $^3S_1$ [4–6], of mesic retardation effects [7], and of the use of energy-dependent potentials (Ref. [7], and references therein), the essential key to solving the problem is a precise determination of the *NN* tensor force component. It is only on this basis that conclusions about the relevance of possible three-body forces—which have currently been invoked to explain the missing binding energy—can be drawn.

For the saturation behavior and the binding of nuclear matter, the tensor force is also dominant (see Ref. [8], and references therein). While the absolute scale for the predicted nuclear-matter binding energy may be questioned, it is clear that the results depend sensitively on the amount of tensor contribution to the basic *NN* interaction. This dependence arises from strong cancellations of contributions from other sources, so that the tensor force finally contributes about 30% to the binding of nuclear matter.

Similar problems as for the triton binding energy are also observed for $3N$ continuum observables. Selected observables in the $3N$ system are prime candidates to look for manifestations of three-body force and/or off-shell effects or to investigate charge-symmetry breaking. However, most of these observables also display a strong dependence on the tensor force [9,10], so that precise and independent information on the latter is absolutely necessary. Vice versa, the determination of the *NN* tensor force from $3N$ continuum observables—which in principle would be very effective because of the strong sensitivities—is hampered by our poor knowledge on three-body force and/or off-shell effects.

Another aspect of interest originates from the study of non-nucleonic degrees of freedom in nuclei. Mesonic degrees of freedom [meson-exchange currents (MEC)] have been shown to be indispensable for a correct description of electromagnetic form factors in the $A = 2,3$ system (see [11], and references therein). While there is no question that MEC corrections are necessary, detailed calculations of these corrections revealed a serious model

dependence with respect to the *NN* potentials used. The choice of *NN* potential influences both the calculation of the electromagnetic process and the calculation of the MEC correction [12]. The origin of this dependence can be traced back to the tensor force, which determines the amount of *S-D* mixing. The MEC contribution to electromagnetic form factors of the $A=2,3$ systems—the observables most sensitive to mesonic degrees of freedom—is of nearly equal size but of opposite sign as the effects of the *S-D* transition [12]. The latitude in P_D as given by different potentials (see above) thus prevents a precise assessment of MEC contributions from electromagnetic processes. The issue will become more important as results at higher momentum transfer will be provided in the near future, where the influence of quark-gluon degrees of freedom is to be explored.

In spite of its unique characteristic, the tensor force is at present still poorly determined. The well-known properties of the deuteron bound state—quadrupole moment, magnetic moment, binding energy, the asymptotic D/S ratio η—determine only the asymptotic behavior at long range and can be easily reproduced by a variety of potentials with values of P_D between 3% and 7%. The connection between the *D*-state probability of light nuclei to the tensor force was recently reviewed by Ericson and Rosa-Clot [13].

In *NN* scattering—the most reliable basis to study the tensor component at positive energies—the tensor force is characterized by the degree of mixing between states of different L. Within a phase-shift parametrization of the *NN* interaction, this mixing is given by the mixing parameters ε_i. For instance, the mixing parameter of lowest order, ε_1, represents the degree of mixing between $^3S_1$ and $^3D_1$, ε_2 between $^3P_2$ and $^3F_2$, and so on. At low energy (i.e., below 100 MeV), the $^3S_1$-$^3D_1$ transition is by far the dominant transition. Since the mixing parameters of odd order, $\varepsilon_1,\varepsilon_3,\varepsilon_5,\ldots$, describe the mixing between states with isospin $T=0$ (isoscalar), they carry a weight factor of 3 as compared to 1 for the isovector transitions.

With respect to energy, by far the most important range for ε_1 is around 50 MeV, which corresponds to the peak of the Fermi momentum distribution in nuclei. The results of nuclear-matter calculations [14] were shown to be insensitive to the specific value of ε_1 at energies above 100 MeV.

By the time of the latest, most comprehensive review on elastic *NN* physics [15], unique phase shifts were reported, with one notable exception: ε_1 was poorly determined between 200 and 500 MeV and between 25 and 50 MeV, where "...measurements of A_{zz} would eliminate present unhealthy correlations between ε_1 and $^1P_1$ and complete the task of achieving a firm phase shift solution" [15]. Around 50 MeV the ε_1 problem, which has been studied specifically by several authors [16,17], is twofold: (1) only higher-order spin observables such as spin correlation or spin transfer parameters in *np* scattering are sensitive to ε_1; (2) these observables in most cases are also sensitive to the other poorly determined quantity, the $^1P_1$ phase. By the time of Bugg's 1981 [15] review, only 3 measurements of spin correlation coefficients in *np* scattering were available below 200 MeV, comprising altogether 12 data points of low statistical accuracy and over restricted angle ranges.

In the present paper, we shall briefly review the new measurements between 15 and 100 MeV which have been performed over the last 10 years. The new data were added to the world database, which was carefully reviewed and updated. The results of the new phase-shift analysis reveal the strong impact of the new data for the determination of ε_1 and confirm the recently observed trend of ε_1 [18] to higher values.

II. THEORETICAL PREDICTIONS FOR ε_1

Throughout the paper we shall use the "nuclear bar" notation by Stapp [19], which is adopted now universally. In contrast with the Blatt-Biedenharn convention [20], this notation gives much simpler relationships between the nuclear phase shifts and the corresponding total phase shifts.

We shall at first focus on the prediction for ε_1 close to threshold. There exist several analytic continuation formulas which relate ε_1 near threshold with bound-state properties of the deuteron or with finite-range parameters (for a review, see Ref. [21], and references therein). The most realistic of these is Wong's formula [22], which involves one-pion exchange, the $^3S_1$ scattering length, and effective range theory. It can be employed for a prediction of ε_1 for energies below 30 MeV if one inserts the deuteron asymptotic D/S ratio η. It was shown in Ref. [21] that ε_1 depends only weakly on this parameter. Using the most recently determined value of η [23], we obtained $\varepsilon_1\simeq 2.4°$ at 25 MeV. This result represents an upper limit as compared to predictions from meson-theory potential models. A survey of modern potentials (since 1970) yields predictions between 1.55° (Bonn *A* [3]) and 2.11° (an early Bonn potential [24]), with the most commonly used models Paris [25], full Bonn [3], and Nijmegen [26] centered between 1.7° and 1.8°.

Within meson theory the tensor force is given almost exclusively by the exchange of π and ρ mesons [3]. The pion is responsible for the long-range component, while the ρ meson produces a short-range contribution of opposite sign. We have studied the latitude of the ε_1 prediction due to small variations in the π,ρ coupling constants. Recent determinations of the πNN coupling constant [27,28] reveal a tendency for weaker coupling (or a softer form factor [29]) with the currently accepted extremes between $g_\pi^2/4\pi=13.3$ [27] and $g_\pi^2/4\pi=14.3$ [30]. For the ρ coupling, there is a certain lattitude in the tensor-to-vector ratio κ, with the lower limit of 3.7 given by the vector-dominance model [31] and the upper limit of 6.3 by the analysis of Hoehler and Pietarinen [32]. It should be noted that the latter analysis used $g_\pi^2/4\pi=14.5$ as input and that the use of a smaller pion coupling constant would shift κ to smaller values. Machleidt and Sammarucca [33] have already shown that the combination of $g_\pi^2/4\pi=13.3$ and $\kappa=3.7$ reproduces the deuteron properties just as well as the conventional combination $g_\pi^2/4\pi=14.4$ and $\kappa=6.1$. Obviously, the deuteron properties only fix certain combinations of π/ρ coupling constants. At energies below 30 MeV, the effect on ε_1 due to variations such as the ones discussed above of $g_\pi^2/4\pi$ and

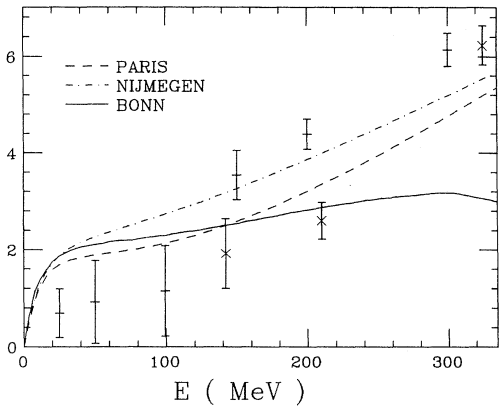

FIG. 1. Potential model predictions for ε_1 up to 325 MeV: full Bonn (solid line), Paris (dashed line), and Nijmegen (dash-dotted line). The symbols represent fixed-energy PSA's before 1990: Ref. [37] (bars) and Ref. [48] (crosses).

κ separately is of the order of a few percent, while the combined effect leaves ε_1 essentially unchanged [34].

In conclusion, phenomenological low-energy parametrization as well as meson-theoretical models fix the low-energy behavior of ε_1 with very small lattitude. We estimate this lattitude to be of the order of 20% at 25 MeV and less at lower energy. It is questionable whether current experiments at low energy will allow a determination of ε_1 at such a level of accuracy [35]. Specifically, a negative value of ε_1 (which resulted from very early phase-shift analyses (PSA's), but see also Ref. [36]) is clearly ruled out. It is suggested to make use of this theoretical constraint in the energy parametrization of PSA's below 25 MeV.

Predictions for ε_1 for energies up to 325 MeV of the most commonly used modern potential models are shown in Fig. 1. A comparison is made to the results of various fixed-energy PSA's which have been performed before 1990 and which did not include the new, precise higher-order polarization data discussed here and in Ref. [18].

It is emphasized at this point that ε_1 (as given by Fig. 1 or similar plots with even larger uncertainties) represented the only (very loose) constraint for modeling the tensor force at positive energies in all modern potentials. By comparison, the deuteron properties placed more stringent limits on the tensor force. Since the deuteron only fixes certain combinations of the π and ρ coupling constants, there is lattitude for ε_1 at higher energies as a result of the different range of the πNN and ρNN interaction. The problem is even more complex because of the uncertainties in the choice of the form factors which have drastic consequences for ε_1 above 30 MeV [3].

III. NEW PHASE-SHIFT ANALYSIS BETWEEN 15 AND 160 MeV

Combined $pp+np$ phase-shift analyses (PSA's) have been performed within the last two decades by the VPI group (0–2 GeV [37]), the Saclay-Geneva group (0–1.6 GeV [38]), the Nijmegen group (0–30 MeV [39]), and by Bugg and Bryan (140–800 MeV [18,40]). Excellent reviews on *NN* phenomenology up to 1 GeV have been given by Bugg [15,41] and Lehar [42].

Although in principle very similar, the approaches of the various groups differ somewhat with respect to the database, the parametrization of the higher partial waves, and the treatment of various corrections. As shall be demonstrated below, the results of the various approaches are quite similar and differ by less than the statistical errors if one starts from roughly the same database and if a similar parametrization of the most significant higher phase shifts (which are invariably taken from some sort of model) is used. The PSA described here made use of the analysis code NNF, details of which are contained in Ref. [37], and references therein.

A. Database

1. *pp* data

For *pp* we have made use of the extensive compilation of the Nijmegen group [43], which cites almost all data published since 1955. However, we did not follow the principle of Ref. [43] to eliminate data sets with very low χ^2 values. (Details on the new precise analyzing power results from PSI at 25 and 39.6 MeV [44, 45] and at 50 MeV [46] which are not used in the analysis of Ref. [43] are contained in Table IV.)

2. *np* data

For *np* we have updated the database following a careful study of the original papers (details on our base are summarized in Table IV) (for previous compilations, see [47,48,38]). The most significant modifications of the old database as well as the new additions shall be discussed in the following.

Data elimination. Elimination of *all* Harwell σ_T [49] and $d\sigma/d\Omega$ [50] data over the whole energy range. Above 50 MeV, the σ_T data are consistently lower by about 3%–4% than three more recent measurements (Ref. [51], and references therein) which quote uncertainties $\leq 1\%$. While σ_T has only minor influence on the determination of the phases discussed here, the situation is very different for $d\sigma/d\Omega$, which heavily dominates the determination of $^1P_1$. Here the Harwell data had an enormous influence. For instance, in the 50 MeV bin (32–68 MeV) where a very conspicuous discontinuity was observed in the energy dependence of $^1P_1$ [37] they represented about 25% of the whole *np* database. In addition, the Harwell data extend from a very forward 7° up to a very backward 173°, an angle range covered by only a few other experiments. The extreme backward angles are most sensitive for the determination of $^1P_1$ [16,52]. The validity of the Harwell data has been questioned before [52] on the basis of PSA studies: Omitting the data resulted in a smooth energy dependence of $^1P_1$ below 100 MeV. Nevertheless, they have been used in all PSA's so far. We strongly recommend the elimination of these data based on the following arguments.

(i) For the backward angular range measured with a liquid-hydrogen/CH_2 target and detection of recoil pro-

tons in a plastic scintillator, no correction was made for the energy dependence of the detection efficiency. For very backward c.m. angles, the energy of the recoil protons is close to the incident neutron energy, whereas around 90° c.m., the recoil proton energy is much lower. Neglecting this effect is serious and introduces distortions of up to 8% (for the angular distribution at 120 MeV) over the angular range $90° \leq \theta_{\text{c.m.}} \leq 173°$. Proper consideration would account for almost all of the discrepancy observed for the ratio $\sigma(173°)/\sigma(90°)$ in comparison to modern potential predictions around 100 MeV and for half the discrepancy observed around 50 MeV.

(ii) For the forward angle measurements with a liquid-hydrogen target and neutron detection in a liquid scintillator, the determination of the neutron detection efficiency was linked to a measurement of σ_T for lead [49]. Because of a general trend of the Harwell σ_T results (for all nuclei measured) to lower values in comparison to other experiments [49,53–55], the forward angle data are thus shifted to too large values.

(iii) After normalization of the backward angle yields to the forward angle cross sections in the overlap region, the angle-integrated cross section was compared to the Harwell σ_T results [49]. Below 65 MeV the integrals were found to be smaller than σ_T. For the final normalization, a procedure was adopted where the very forward angle data were kept fixed and the data at larger angles were lowered to yield agreement with σ_T.

Altogether, the effects mentioned produce angular distributions which are qualitatively too high at forward angles and too low at backward angles. As an example, we show in Fig. 2 a comparison between the Harwell data at 47.5 MeV and the Davis [56] and Karlsruhe [57] data at 50 MeV. As expected from the discussion above, the Harwell results are higher by about two standard deviations at forward angles and lower by about the same amount at backward angles. The Davis and Karlsruhe data, on the other hand, are mutually consistent and agree with the potential predictions within errors.

Renormalization. We renormalized a number of old cross-section data which were originally normalized to

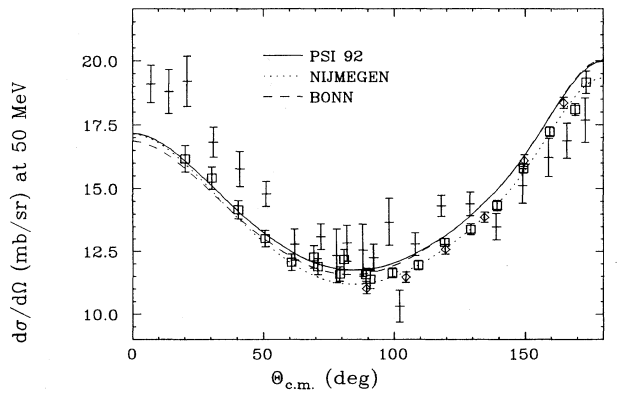

FIG. 2. Differential cross section at 50 MeV. The solid, dotted, and dashed lines represent the prediction of the present PSA, of the Nijmegen, and of the full Bonn potentials. Open squares (diamonds) show the data of Ref. [56] (Ref. [57]) at 50 MeV; bars the Harwell data [94] at 47.5 MeV.

experimental σ_T values. Modern σ_T values are in general higher by up to 5%. Also, we have raised in some cases the normalization uncertainties (for cross sections as well as polarizations) which seemed unreasonably small in hindsight when comparing them with newer, more precise data.

New data. The LASL σ_T data [51,58] supersede the erroneous Harwell data. We used *all* data which were subject to a common normalization. New differential cross-section data in the backward hemisphere between 20 and 100 MeV were provided by Karlsruhe [57], Louvain-la-Neuve [59], and Uppsala [60], new analyzing power data by TUNL at 16.9 MeV [61], Pretoria at 21.9 MeV [62], Wisconsin at 25 MeV [63], and our group at 68 MeV [64].

The new input relevant for the determination of ε_1 is provided by the following 5 experiments (comprising 68 data points of quality much superior to the 12 old A_{yy} data used in all PSA's before 1990).

The Bonn group has measured the polarization transfer coefficient $K_y^{y'}(130°)$ at 17.4 MeV [65] and 25.8 MeV [66]. This observable is highly sensitive to ε_1 and quite insensitive to $^1P_1$ [16]. The result at 17.4 MeV ($K_y^{y'}=0.15\pm0.03$) is about two standard deviations lower than the corresponding potential model predictions [$K_y^{y'}=0.203$ (0.216) for the Bonn (Paris) potential]; while the result at 25.8 MeV ($K_y^{y'}=0.203\pm0.011$) is consistent with the potential predictions [$K_y^{y'}=0.182$ (0.195) for the Bonn (Paris) potential].

The Karlsruhe group [67] used a neutron beam with a continuous energy distribution [68] to measure simultaneously five angular distributions of the transverse spin correlation coefficient A_{yy} between 18 and 50 MeV. This set of data complements the other Karlsruhe measurements of A_y [69] and $d\sigma/d\Omega$ [57] over the same energy range. Within the angle range measured ($60° \leq \theta_{\text{c.m.}} \leq 130°$), A_{yy} is sensitive to both phases ε_1 and $^1P_1$ (see Fig. 3). The region below 60°, where the sensitivity to ε_1 is highest and almost negligible to $^1P_1$, could not be measured since the background contribution from target material other than hydrogen became overwhelming. The polarized target was a 4-cm-thick slab of hydrogenated titanium powder, polarized by "brute force" in a 9 T magnetic field [70]. The experiment was based on the detection of scattered neutrons in an array of liquid scintillation counters. Apart from the absolute calibration of the polarization of the neutron beam and proton target, the most critical problems were the proper background subtraction, the determination of the correct energy and angle ranges, and the proper correction for multiple-scattering effects. In view of the latter problems, we have not used a common normalization uncertainty for all A_{yy} data. Figure 3 shows as an example the results at 25 MeV which exhibit the smallest statistical errors. Also shown are the old Los Alamos data at 23.1 MeV [71] as well as several Bonn predictions to demonstrate the sensitivity of A_{yy} to ε_1 and $^1P_1$.

At 67.5 MeV our group [72] measured the longitudinal spin correlation coefficient A_{zz} for $105° \leq \theta_{\text{c.m.}} \leq 170°$ with typical statistical accuracies of 0.008 (see Fig. 4). At

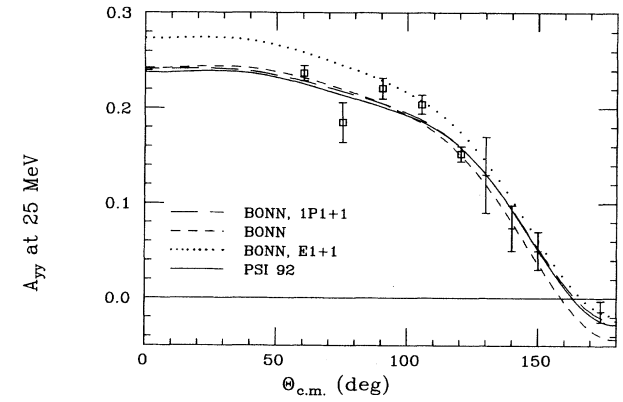

FIG. 3. Transverse spin correlation parameter A_{yy} at 25 MeV. The solid line represents the prediction of the present analysis, while the short-dashed (long-dashed and dotted) curves show full Bonn predictions (with a modification of ε_1 and $^1P_1$ by 1°). Open squares show the data of Ref. [67] at 25 MeV and bars the Los Alamos data [71] at 23.1 MeV.

backward angles A_{zz} displays a strong sensitivity to ε_1 [16,17]. The sensitivity to $^1P_1$ is still pronounced, being $\sim 70\%$ of that for ε_1. In contrast with the Karlsruhe experiment, we employed a thin polarized target (3 mm of frozen butanol, dynamically polarized) and a "quasi-monoenergetic" [2.3 MeV full width at half maximum (FWHM)] neutron beam [73]. As a consequence, the recoil protons displayed a clear signature in the scintillation counter energy spectra with the background amounting to typically 10%. Information on the proton trajectories was provided by three multiple wire proportional chambers (MWPC's). The critical problems of this experiment were the absolute calibration of the polarization of the neutron beam [74] and the proton target [75]. The overall normalization error was 6%. Around the zero crossing at 152°, the normalization uncertainties due to the beam and target polarizations are negligible. We have exploited this fact in a separate analysis where we replaced $A_{zz}(\theta)$ by the zero-crossing datum. The zero crossing was determined very accurately from a fit to the data above 130°. The uncertainty at the zero crossing was chosen in such a way as to obtain the same error for ε_1 from the PSA. In this way the zero-crossing point exerts the same statistical weight as $A_{zz}(\theta)$ in the standard analysis. Relative to the nominal solution, $\varepsilon_1/^1P_1$ changed by only 0.10°/0.40° (compare also to Table I), even if we take into account the 0.5° uncertainty of the angle determination. We consider this to be strong evidence for the reliability of the polarization normalizations. It is very important to note that the zero-crossing predictions of Bonn and Paris potentials lie within the angle range given by the experiment; thus there is no conflict between our measurement and these models. The Nijmegen prediction, on the other hand, is off by 7°, only a part of which can be explained as due to the anomalous Nijmegen $^1P_1$ value.

A measurement of A_{zz} at forward angles, where the sensitivity to ε_1 is largest and negligible to $^1P_1$, is in progress by the same group at PSI [76].

The spin-dependent total cross section difference $\Delta\sigma_L$ in the interaction of a 66 MeV longitudinally polarized neutron beam with a longitudinally polarized proton target was measured recently at PSI [77]. At this energy $\Delta\sigma_L$ is roughly 3 times more sensitive to ε_1 than to $^1P_1$. The sensitivity is even more pronounced at lower energy; a program to measure $\Delta\sigma_L$ and $\Delta\sigma_T$ is presently being carried out at TUNL [35]. At PSI we measured the spin-dependent attenuation of the longitudinally polarized neutron beam in a 2.4-cm-thick longitudinally polarized proton target. The neutrons were observed in a stack of thin plastic scintillators, requiring coincidences between two scintillators in order to reduce the sensitivity to constant background and gain shifts. Special attention was given to studying the effects of spin-correlated modulations (intensity, position, phase space, timing) of the incident proton beam. Besides statistics, the dominant systematic errors are due to the uncertainties in the polarization of the neutron beam (4%) and the proton target (4%), as well as in the determination of the hydrogen target thickness (1%) [78].

The result $\Delta\sigma_L = -26.5 \pm 1.2 \pm 1.6$ mb (where the first uncertainty corresponds to the statistical error and the second to the systematic error) is considerably more positive than the predictions of the potential models [−29.9 mb (full Bonn), −33.8 mb (Paris), −32.2 mb (Nijmegen)], or of old PSA's which do not contain the new higher-order spin data (−42.1 mb [37], −28.9 mb (Saclay S80 [38])).

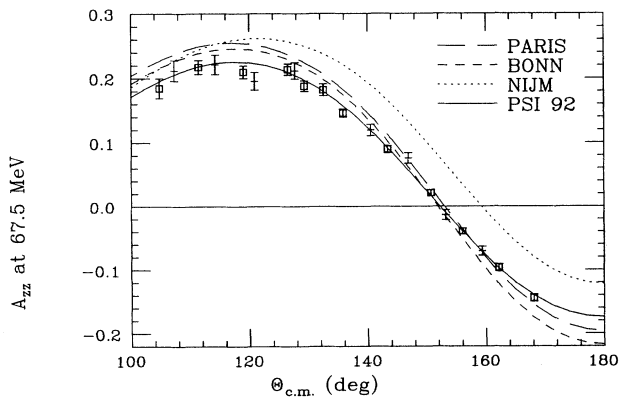

FIG. 4. Longitudinal spin correlation parameter A_{zz} at 67.5 MeV. The solid line represents the prediction of the present analysis (multiplied by the fitted renormalization factor 0.94), while the short-dashed, long-dashed, and dotted curves represent the predictions of Bonn, Paris, and Nijmegen. The data are from PSI [72]; the different symbols represent the results of two run times.

B. PSA procedure

The energy range 15–160 MeV was divided into four bins, roughly corresponding to the binning of previous PSA's to facilitate comparison. Details of the binning are given in Tables I and II.

Within each energy bin, we proceeded as follows:

TABLE I. Results of our PSA at the nominal energies of 25 and 50 MeV. Δ, N_i^{pp}, N_i^{np}, N_{df}, and χ^2_ν denote the (*pp-np*) charge splitting, the number of *pp* data, number of *np* data, total number of degrees of freedom, and reduced χ^2. All $T=1$ phases are given for the *np* case; the corresponding *pp* phases can be calculated from $\delta(pp)=\delta(np)+\Delta$. Values set in parentheses represent fixed parameters.

	25 MeV (15–35 MeV)			50 MeV (32–68 MeV)	
Phase	13 par	*np* only	Δ	13 par	Δ
$^1S_0$	50.00(0.11)	49.9(1.0)	−1.65	40.10(0.09)	−1.03
$^3P_0$	8.75(0.10)	9.1(0.9)	−0.32	11.37(0.10)	−0.29
$^1P_1$	−6.29(0.35)	−5.9(0.4)		−9.46(0.22)	
$^3P_1$	−5.23(0.06)	−5.3(0.6)	0.20	−8.51(0.04)	0.27
$^3S_1$	81.14(0.46)	81.5(0.6)		62.75(0.34)	
ε_1	1.74(0.22)	1.6(0.4)		2.80(0.25)	
$^3D_1$	−3.14(0.21)	−3.1(0.3)		−7.17(0.08)	
$^1D_2$	0.70(0.03)	1.0(0.2)	−0.01	1.70(0.03)	−0.05
$^3D_2$	4.36(0.39)	4.2(0.6)		9.82(0.17)	
$^3P_2$	2.62(0.02)	2.7(0.4)	−0.17	6.09(0.02)	−0.27
ε_2	−0.82(0.04)	(−0.88)	0.01	−1.67(0.03)	0.01
$^1F_3$	−0.45(0.10)	(−0.44)		−1.13(0.11)	
ε_3	0.71(0.18)	(0.58)		1.52(0.12)	
$^3F_3$	(−0.25)	(−0.25)		(−0.71)	
$^3G_4$	(0.18)	(0.18)		(0.76)	
P_C	0.69(0.02)	0.76(0.18)		1.81(0.02)	
P_{LS}	0.94(0.02)	0.94(0.27)		2.77(0.02)	
P_T	−2.49(0.02)	−2.56(0.17)		−3.78(0.02)	
D_C	0.84(0.14)	0.80(0.21)		1.88(0.06)	
D_{LS}	0.12(0.04)	0.12(0.10)		0.28(0.02)	
D_T	1.82(0.12)	1.75(0.20)		4.11(0.05)	
χ^2/N_i^{pp}	135/110			224/223	
χ^2/N_i^{np}	271/318	269/318		339/299	
χ^2/N_{df}	406/363			562/455	
χ^2_ν	1.12			1.23	

Given a certain start solution, being any one of the potential models Bonn [3,6], Paris [25], Nijmegen [26], or the energy-dependent solution V350 of the 1990 SAID data file [79] (which already included the new spin correlation data above 200 MeV from TRIUMF [80] and IUCF [81]), we first investigated the energy dependence of the phases. Within each bin the phases are parametrized as linear functions of energy with the gradient given at the nominal energy. In certain cases this is a rather crude approximation (e.g., for $^3P_0$ around 60 MeV, $^1D_2$ around 100 MeV) and has to be considered as a source of systematic uncertainty. For the cases mentioned above, we introduced a "reasonable" gradient which was optimized for minimum χ^2. We have also studied the effects of varying the gradients of the leading phases within the lattitude given by the various start solutions. We found that the scatter of the fitted phases was well within the statistical errors of the fit.

In the next step, we studied the charge splittings for the $T=1$ phases. Via data analysis a clean determination of *np* and *pp* phases could only be obtained in the 25 MeV bin where there is sufficient data to allow for a ten-parameter fit to *np* data only. Results are given in the third column of Table I; the differences $\Delta=\delta(pp)-\delta(np)$ are presented in the last column of Table III. We also attempted to fit the splittings in the full analysis. This often led to an improvement of χ^2; however, the resulting values differed widely from theoretical predictions, and above all, they displayed no consistent behavior as a function of energy. Obviously, without additional constraint about the energy dependence the data do not allow for a reliable determination of the splittings.

From a theoretical point of view, there exist several formulas in the literature for calculating the splittings. In the VPI analyses [37], the splittings are described by a Coulomb penetration factor, taking also into account the mass difference between the neutral and charged pions. The TRIUMF analyses [18,40,48] use the Graz prescription [82]. Both calculations assume charge independence of the pion coupling constant and arrive at roughly the same values. For $^1S_0$ we used the difference between the Bonn and Paris predictions, the Bonn $I=0$ phases being obtained from a fit to *np* data and the Paris ones from *pp* data. This splitting is strongly supported by our 25 MeV analysis (see Table III). For the higher L splittings, we have adopted the Arndt-Hyslop-Roper splittings. It should be pointed out that the charge splittings have only negligible influence on the determination of the phases, even for very large variations.

For a solution to be considered reliable, we used the following "stability" criteria: The fitted phases should be within the error margin given by the parameter uncertainties of the fit irrespective of (1) which of the four start solutions (Paris, Bonn, Nijmegen, and the energy-

TABLE II. Results of our PSA at the nominal energies of 100 and 140 MeV. The symbols have the same meaning as in Table I.

Phase	100 MeV (80–120 MeV) 10 par	Δ	140 MeV (120–160 MeV) 12 par	Δ
$^1S_0$	24.74(0.37)	−0.48	17.16(0.37)	−0.34
$^3P_0$	11.33(0.91)	−0.14	6.52(0.28)	0.03
$^1P_1$	−14.55(0.70)		−16.96(0.54)	
$^3P_1$	−14.25(0.20)	0.35	−17.18(0.08)	0.41
$^3S_1$	42.83(0.44)		31.09(0.45)	
ε_1	4.14(0.56)		3.22(0.38)	
$^3D_1$	−11.46(0.26)		−15.12(0.31)	
$^1D_2$	4.03(0.07)	−0.14	4.98(0.08)	−0.23
$^3D_2$	16.73(0.52)		22.66(0.42)	
$^3P_2$	10.64(0.18)	−0.38	13.93(0.06)	−0.45
ε_2	(−2.85)	0.05	−2.79(0.05)	0.07
$^1F_3$	(−2.27)		(−3.00)	
ε_3	(3.68)		(4.61)	
$^3F_3$	(−1.61)		−2.15(0.05)	
$^3G_4$	(2.28)		(3.55)	
P_C	2.42(0.16)		2.74(0.05)	
P_{LS}	6.10(0.17)		9.01(0.06)	
P_T	−5.28(0.13)		−5.45(0.04)	
D_C	4.32(0.18)		5.40(0.15)	
D_{LS}	0.84(0.06)		0.82(0.06)	
D_T	6.63(0.16)		9.04(0.14)	
χ^2/N_i^{pp}	112/114		256/265	
χ^2/N_i^{np}	338/271		264/206	
χ^2/N_{df}	450/373		520/432	
χ^2_ν	1.21		1.20	

dependent solution V350 [79]) was used, (2) small changes in the energy dependences of the phases (within the lattitude given by the start solutions), and (3) small variations of the number of fit parameters.

The solutions at 25 and 50 MeV were found to be highly stable, while the ones at 100 and 140 MeV showed instability to tests 1 and 3 (see the discussion below).

Obviously, the unstable behavior at 100 and 140 MeV reflects the larger number of contributing partial waves as well as the small database, which in addition is not specific enough for the determination of, e.g., ε_1: There is no single *np* spin observable datum of higher order between 70 and 160 MeV.

TABLE III. Charge splittings Δ at 25 MeV. See text for explanation.

Phase	$\Delta=\delta(pp)-\delta(np)$ Nijmegen	Bochum	PSI
$^1S_0$	not given	not given	−1.6(1.0)
$^3P_0$	−1.5	−2.14	−0.7(0.9)
$^3P_1$	0.5	0.21	0.2(0.6)
$^1D_2$	not given	not given	−0.2(0.2)
$^3P_2$	−0.3	−0.13	−0.3(0.4)

IV. RESULTS

The results of our analysis are given in Tables I and II. The most important isoscalar phases are displayed in Figs. 5 and 6 as a function of energy. The errors given in parentheses represent the diagonal elements of the error matrix. We have also verified that the errors obtained in this way coincide with the parameter latitudes given by the usual $\chi^2_{\min}+1$ criterion for simultaneous variation of all other parameters. Statistical information on the solutions—total χ^2, number of data points, number of degrees of freedom, and reduced χ^2_ν—are given at the end of Tables I and III. Statistical information on the data itself is contained in Table IV.

Since in the vicinity of zero energy the phases are well constrained theoretically (see Sec. II above), the good agreement with theory at 25 MeV is taken as an indication for the reliability of the low-energy solution. Specifically, even phases with rather small values ($^1F_3, \varepsilon_3$) could be determined reliably. It should be pointed out that the extended database allowed for a *more accurate* determination with a *larger* number of fit parameters as compared, e.g., with the 1987 analysis of Arndt, Hyslop, and Roper [37]. The uncertainties are smaller for all phases; the most significant improvement is observed for the isoscalar phases, e.g., a factor of almost 3 for ε_1 and $^1P_1$ at 50 MeV.

A critical problem of several previous PSA's was the unsatisfactory database, resulting in a strong dependence on specific data sets (see the above discussion on the Harwell data) or in ambiguities (see, e.g., Ref. [83]). With regard to the determination of ε_1, we have analyzed the effects of eliminating certain data sets. For the 25 MeV bin, we find that omitting the Karlsruhe A_{yy} [67] results yields $\varepsilon_1/^1P_1 = 1.43°\pm0.42°/-6.06°\pm0.57°$, while omitting the Bonn [66,65] and Los Alamos [84] data yields $1.71°\pm0.23°/-5.90°\pm0.53°$. For the 50 MeV bin, we find that omitting the Karlsruhe A_{yy} [67] results yields

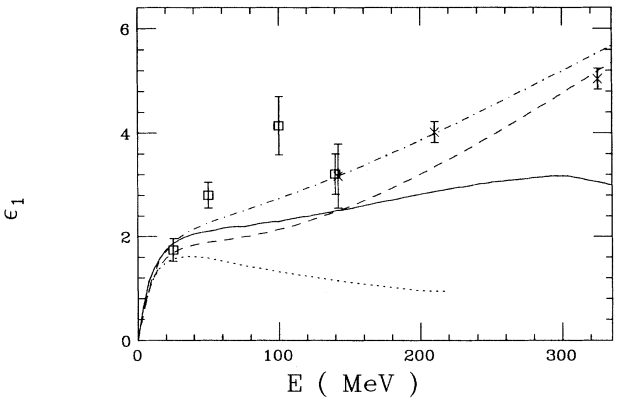

FIG. 5. ε_1 between 0 and 325 MeV. Several potential model predictions (solid line, Bonn; dashed line, Paris; dash-dotted line, Nijmegen; dotted line, Bonn *A*) are compared to the two most recent PSA's, which include the new spin correlation data: crosses (Ref. [40]) and open squares (this work). The errors represent the statistical uncertainty of the fits; see, however, text for the consideration of systematic uncertainties.

$\varepsilon_1/{}^1P_1 = 3.04° \pm 0.30° / -9.70° \pm 0.25°$, while omitting the PSI A_{zz} [72] and $\Delta\sigma_L$ [77] data yields $2.34° \pm 0.46° / -8.66° \pm 0.49°$. Thus at both energies the results drawn from four independent experiments are mutually consistent. Given previous experience with the determination of e.g., ${}^1P_1$ (i.e., the scatter between different PSA's), we estimate the systematic uncertainty for critical phases such as ε_1 and ${}^1P_1$ to be of the same order of magnitude as the statistical uncertainty.

In contrast with the situation at 25 and 50 MeV, the situation at energies ≥ 100 MeV is still unsatisfactory. The solution at 100 MeV is very unstable against choice of the start solution, e.g., higher partial waves. For instance, ε_1 becomes as large as 7° if one starts from V350, while the recommended solution is obtained with any of the potential models Bonn/Paris or Nijmegen. The difference amounts to 3° or almost four standard deviations. The most disturbing fact, however, is that the presently obtained high value of ε_1 is entirely due to the inclusion of the new Uppsala cross-section data at 96 MeV [60]. Without these, ε_1 is shifted down to lower values by 4° consistently for all start solutions and shows agreement with the 1987 analysis of Arndt, Hyslop, and Roper (see Fig. 1). Figure 7 shows the new data together with predictions of potential models and of our PSA. If these data survive critical inspection, they lend strong support to a high ε_1 level since all other phases are smooth with energy and in good agreement with the potential models. Nevertheless, it is clear that higher-order spin data are highly desirable for a direct access to ε_1. In view of this problem, we estimate the overall uncertainty of ε_1 at this energy to be at least twice the statistical error of the fit.

At 140 MeV no new data have been obtained since 1985. Therefore this bin represents a good test case to compare the various PSA's which have been performed

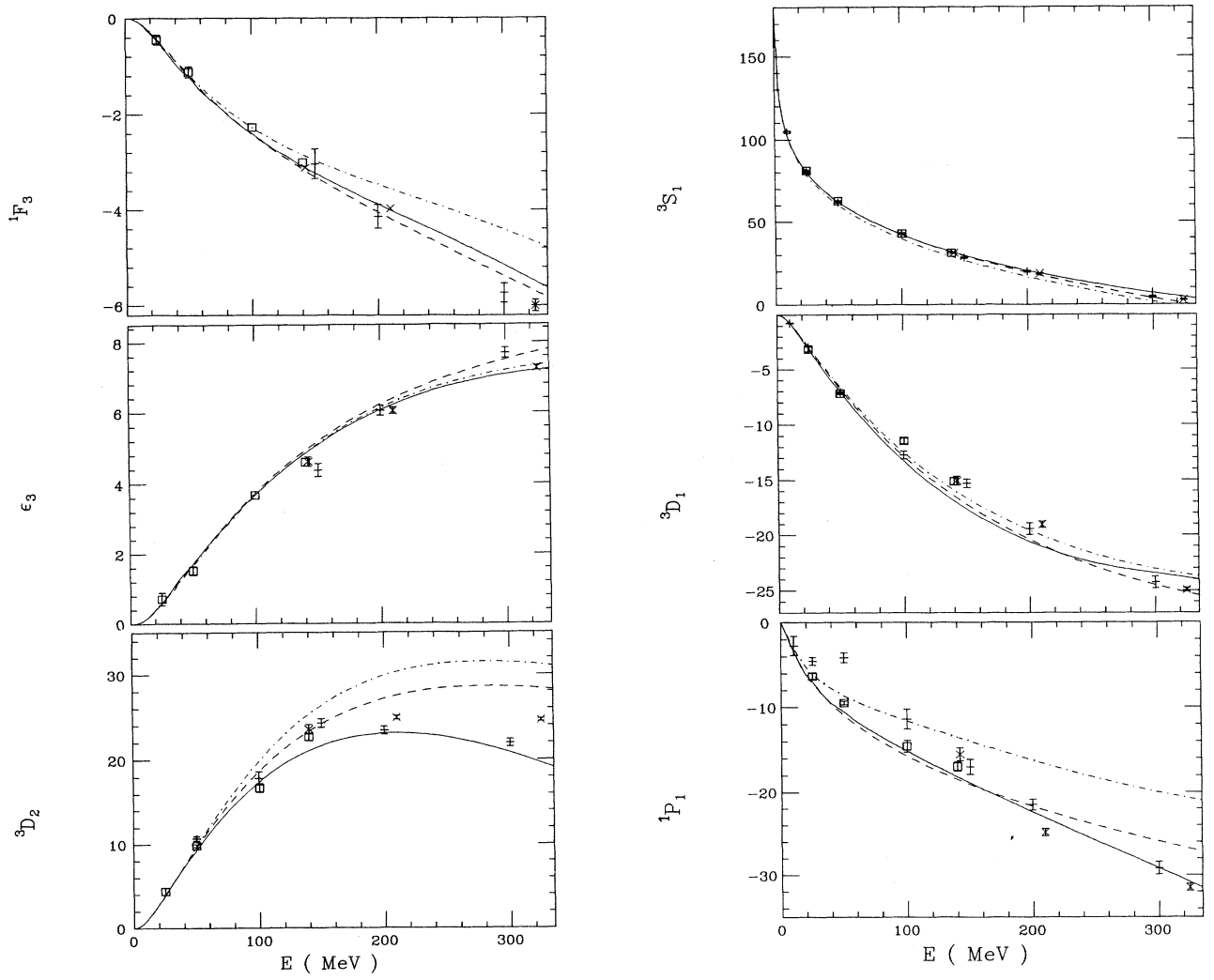

FIG. 6. Leading isoscalar phase shifts in the energy range between 0 and 325 MeV. Curves represent potential model predictions (solid curve, full Bonn; dashed curve, Paris; dash-dotted curve, Nijmegen), the symbols stand for the fixed-energy PSA's of Ref. [37] (bars), Ref. [40] (crosses), and this analysis (open squares).

TABLE IV. Information on the new *pp* data and on the full *np* database. Rejected data are not given. The second, third, and fourth column specifies the number and type of data. M is a measure of the quality of the data and is defined as χ^2_{tot}/(number of data points) for a given set of data. The predicted normalization corresponds to the fitted normalization parameter and is to be compared to the normalization error which was either given by the experiment or estimated.

T_{lab} (MeV)	σ	First order	Second order	M	Normal error (%)	Predicted norm	Ref.	Comment
				New *pp* data				
25.7		24 P		2.16	2	1.00	[45]	
39.4		7 P		6.50	2	0.98	[45]	
50.0		10 P		0.51	2	1.01	[46]	
				np data				
15.5–42.2	21 σ_t			1.24		1.01	[58]	
15.7	16 σ			0.69	float	1.03	[97]	
15.9–20.0	$3\sigma_t$			0.80			[98]	
16.0		1 P		0.64			[99]	
16.2		3 P		0.22			[100]	
16.4		3 P		0.98	9	1.00	[101]	
16.4		4 P		0.53	10	0.97	[102]	a
16.8		1 P		0.08			[103]	
16.9		4 P		0.84	6	0.94	[104]	
16.9		11 P		1.51	2	1.00	[61]	
16.9		4 P		0.11	1	1.00	[61]	
17.0		6 P		0.68	2	1.00	[69]	
17.4			1 $K_y^{y'}$	2.07			[65]	
17.8–29.0	5 σ_t			1.36	2	0.99	[54]	
19.0		6 P		0.70	3	1.00	[69]	
19.0			5 A_{yy}	0.22	6	1.01	[67]	b
19.6–27.9	$3\sigma_t$			0.51	0.1	1.00	[105]	
20.5		9 P		0.76	19	1.13	[106]	
21.1		6 P		1.23	20	1.29	[104]	c
21.6		7 P		0.12	10	1.01	[102]	c
21.6		5 P		0.95	4	1.03	[62]	
22.2	5 σ			0.26	3	1.00	[57]	d
22.0			5 A_{yy}	0.57	6	1.03	[67]	b
22.0		8 P		1.41	3	1.02	[69]	
22.5	12 σ			0.53	float	0.98	[107]	
22.5–3.19	$2\sigma_t$			0.90	2	0.99	[107]	
23.1		6 P		0.73	4	0.99	[108]	
23.1		2 P		0.33	20	0.91	[103]	
23.1			4 A_{yy}	0.18			[71]	
23.7		4 P		0.42	11	0.95	[101]	
24.0	4 σ			0.50	float	0.99	[109]	
24.0	2 σ			0.16			[110]	
24.0	4 σ			1.00	5	0.97	[111]	
24.6–59.4	8 σ_t			0.07	3	1.00	[112]	
25.0			5 A_{yy}	1.68	6	1.03	[67]	b
25.0		16 P		1.77	3	0.92	[63]	
25.0		8 P		0.82	3	1.01	[69]	
25.0	5 σ			0.46	3	0.98	[57]	d
25.3	1 σ			0.03	1	1.00	[113]	
25.8			1 $K_y^{y'}$	0.98			[66]	
25.8	8 σ			0.54	3	0.99	[56]	
25.8	8 σ			0.51	3	0.99	[56]	
27.2	5 σ			0.29	float	1.00	[109]	
27.4	5 σ			0.50	3	0.98	[57]	d
27.5			5 A_{yy}	2.02	6	0.99	[67]	b
27.5		8 P		1.86	3	1.02	[69]	
29.6		3 P		0.43	10	1.03	[103]	
29.6		11 P		0.16	5	1.01	[114]	
29.9	5 σ			0.63	3	0.99	[57]	d
30.0			5 A_{yy}	2.70	6	0.95	[67]	b

TABLE IV. (*Continued*).

T_{lab} (MeV)	σ	First order	Second order	M	Normal error (%)	Predicted norm	Ref.	Comment
30.0		9 P		1.36	8	0.95	[106]	
30.0		3 P		0.74	8	0.98	[106]	
30.0		8 P		0.84	3	0.99	[69]	
31.1	1 σ			0.01	1	1.00	[113]	
32.9	6 σ			0.38	3	0.99	[57]	d
33.0		8 P		0.81	3	1.03	[69]	
33.0			5 A_{yy}	1.10	6	1.02	[67]	b
35.8	6 σ			0.81	3	1.01	[57]	d
36.0		8 P		0.64	3	1.01	[69]	
36.0			5 A_{yy}	0.74	6	0.99	[67]	b
39.7	6 σ			1.56	3	1.01	[57]	d
40.0	3 σ			0.81	5	0.99	[59]	e
40.0		9 P		0.79	11	1.02	[106]	f
40.0		6 P		0.60	11	1.05	[106]	f
40.0		8 P		1.69	3	1.00	[69]	
40.0			5 A_{yy}	1.08	6	0.97	[67]	b
45.0–159.0	36σ_t			1.51	1	0.99	[51]	
45.0	3σ			1.11	5	0.99	[59]	e
50.0			5A_{yy}	1.85	6	0.93	[67]	b
50.0		8 P		1.97	3	1.04	[69]	
50.0		9 P		0.19	5	1.01	[106]	
50.0		6 P		0.83	5	0.99	[106]	
50.0		9 P		1.12	4	0.95	[115]	
50.0		7 P		2.33	4	0.98	[116]	
50.0	3σ			0.36	5	0.99	[59]	e
50.0	6 σ			1.86	3	0.97	[57]	d
50.0	8 σ			0.34	5	0.99	[56]	g
50.0	12 σ			0.89	5	0.97	[56]	g
50.0			4 A_{yy}	0.50	25	0.73	[117]	
50.0			4A_{yy}	1.33	8	0.92	[118]	
55.1	3σ			0.66	5	0.99	[59]	e
58.8	9 σ			0.61	10	0.93	[96]	b
60.0		9 P		0.61	15	0.86	[106]	f
60.0		7 P		1.68	15	0.90	[106]	f
61.0	2σ			0.39	5	0.99	[59]	e
62.2	3σ			0.86	5	0.99	[59]	e
63.1	19 σ			2.47	3	1.00	[119]	i
65.0	3 σ			2.01	5	0.99	[59]	e
66.2			1 $\Delta\sigma_t$	2.48	6.0	0.93	[77]	
67.5			20 A_{zz}	0.98	6.0	0.93	[72]	
67.5		31 P		0.86	4.0	1.00	[64]	
67.5	11 σ			1.56	10	0.91	[96]	h
80.0		9 P		0.43	15	0.89	[106]	f
80.0		7 P		0.38	15	0.98	[106]	f
86.5	11 σ			1.54	10	0.85	[96]	h
88.0–150.9	6 σ_t			0.19	2	1.00	[120]	
90.0		9 P		0.64	15	0.88	[106]	f
90.0		7 P		0.35	15	0.96	[106]	f
90.0	9 σ			1.16	3	1.00	[121]	
90.0	4 σ			0.77	15	1.10	[122]	
90.0	16 σ			3.20	3	1.01	[123]	
90.0	18 σ			1.76	float	0.90	[95]	
91.0	23 σ			1.50	3	0.98	[124]	j
93.0	6 σ			1.24	3	0.97	[125]	
95.0		15 P		2.19	8	0.91	[125]	
96.0	32 σ			1.09	4	0.99	[60]	
96.8	11 σ			1.31	10	0.89	[96]	h
100.0		9 P		0.37	7	1.00	[106]	
100.0		7 P		0.51	7	1.01	[106]	

TABLE IV. (*Continued*).

T_{lab} (MeV)	σ	First order	Second order	M	Normal error (%)	Predicted norm	Ref.	Comment
105.0	7 σ			0.35	8	1.08	[126]	
107.6	11 σ			1.42	10	0.90	[96]	h
110.0		8 P		1.19	10	1.01	[106]	
110.0		7 P		1.25	10	1.04	[106]	
118.8	11 σ			1.25	10	0.88	[96]	h
120.0		7 P		0.42	15	0.98	[106]	
120.0		7 P		0.55	15	1.05	[106]	
125.9–145.7	2 σ_t			0.29	1	0.99	[127]	
126.0		6 P		0.62	10	1.07	[128]	
128.0		10 P		1.26	10	1.04	[129]	
128.0	10σ			0.76	7	0.97	[129]	
128.0			1 D_t	1.09			[130]	
128.0			5 D_t	1.96			[131]	
129.0	15 σ			0.76	7	0.95	[120]	
129.0	9 σ			0.49	16	1.02	[132]	
129.0	16 σ			1.24	7	0.98	[132]	
130.0	14 σ			0.67	5	0.99	[133]	k
130.5	11 σ			1.16	10	0.94	[96]	h
137.0	7 σ			0.60	5	0.95	[126]	
140.0		14 P		1.36	4	0.98	[134]	
142.8	11 σ			0.26	10	0.96	[96]	h
150.0	16 σ			0.98	7	0.97	[120]	
152.0	13 σ			1.82	float	1.06	[135]	
155.4	11 σ			2.80	10	0.92	[96]	h
156.0	19 σ			3.49	10	1.02	[136]	l

[a]Multiplied by 0.76 according to Brock *et al.*, Nucl. Phys. **A361**, 368 (1981).
[b]Estimated normalization error.
[c]As given by Ref. [62].
[d]Normalization error raised to a more realistic 3%.
[e]Original cross-section ratios were converted into angular distributions normalized to the Bonn prediction at 90°.
[f]Normalization error was raised based on a critical inspection of Ref. [106].
[g]Normalization error was increased because of neglected neutron detection efficiency uncertainty.
[h]Uncertainties increased at higher angles to include detection efficiency error.
[i]Multiplied by 1.036 to account for normalization to modern σ_t values.
[j]Multiplied by 1.056 to account for normalization to modern σ_t values.
[k]Multiplied by 1.05 to account for normalization to modern σ_t values.
[l]Multiplied by 1.078 to account for normalization to modern σ_t values.

since. The comparison between Refs. [37, 18, 40] and our solution (see also Fig. 1) reveals a scatter which, e.g., for ε_1 corresponds to the statistical errors quoted by the different analyses.

At low energy the parametrization in terms of central, spin-orbit, and tensor phase combinations is more simple, yields more physical insight, and should therefore present a more rigorous test with respect to potential models. Vice versa, theory may provide guidelines which are more reliable for the combinations than for the individual phase shifts, a feature which has been used by several previous PSA's as an additional constraint (see, e.g., Ref. [18]). For the P and D waves, the combinations are given in Tables I and II and plotted in Figs. 8 and 9 together with the results of other PSA's and of Bonn and Paris. In general, the phase combinations show a smooth energy dependence; minor problems exist at 100 MeV for P_C and at 100 and 140 MeV for D_{LS}. The comparison with the potential models yields some preference for Bonn, except for D_C, which lies between both models.

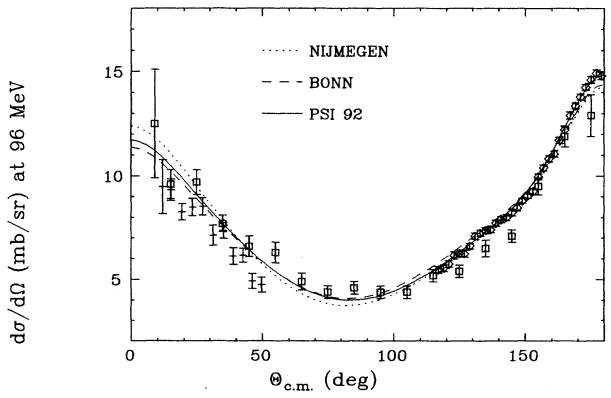

FIG. 7. Differential cross section at 96 MeV. The new data of Ref. [60] at 96 MeV (diamonds) are compared to the results of Ref. [95] at 90 MeV (squares) and of Ref. [96] at 96.8 MeV (bars). The solid, dashed, and dotted curves represent the predictions of this analysis and of the Bonn and Nijmegen potentials.

V. DISCUSSION

A. Tensor force

We shall now discuss the results with respect to the tensor force. The largest and most important difference with respect to the potential predictions or to previous PSA's occurs for ε_1 and $^1P_1$ in the 25–100 MeV range. The impact of the new data is shown by the striking reduction, by a factor of 3, of the uncertainties in ε_1 and $^1P_1$. The new value of $^1P_1$ ($-9.5°\pm0.2°$) at 50 MeV is much more negative than the recent value of Ref. [37] ($-4.1°\pm0.6°$) and essentially removes the notorious discontinuity at 50 MeV caused by the Harwell data. Nevertheless, it is still more positive than the Bonn ($-10.5°$) and Paris ($-10.9°$) predictions. There is no particular data set responsible for this behavior. What is hence urgently needed is new, precise measurements of $d\sigma/d\Omega$ over the whole angular range, obtained with good absolute normalization.

ε_1 at 50 MeV is determined by the Karlsruhe A_{yy} and PSI A_{zz} and $\Delta\sigma_L$ results, with a strong statistical dominance of the A_{zz} data. The value of ε_1 ($2.80°\pm0.25°$) is significantly higher than the predictions of the potential models and of the 1987 analysis of Arndt, Hyslop, and Roper [37]. One should bear in mind that this determination is closely linked to the value of $^1P_1$. More positive values of $^1P_1$ require larger values of ε_1 in order to fit A_{zz}. Although the new value of $^1P_1$ is much closer to the potential model predictions than previous PSA's, the observed discrepancy is a cause of concern because of this correlation. As pointed out above, there is strong evidence provided by the zero-crossing analysis that the A_{zz} data are not responsible for the discrepancy in ε_1. The

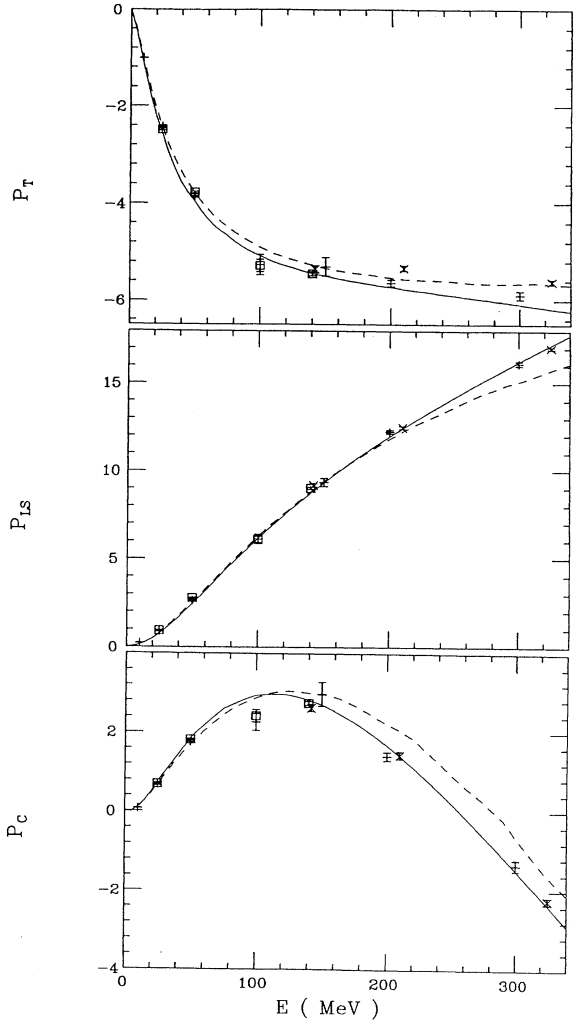

FIG. 8. Central, *LS*, and tensor phase combinations of the *P* waves. Curves represent potential model predictions (solid curve, full Bonn; dashed curve, Paris); the symbols stand for the fixed-energy PSA's of Ref. [37] (bars), Ref. [40] (crosses), and this analysis (open squares).

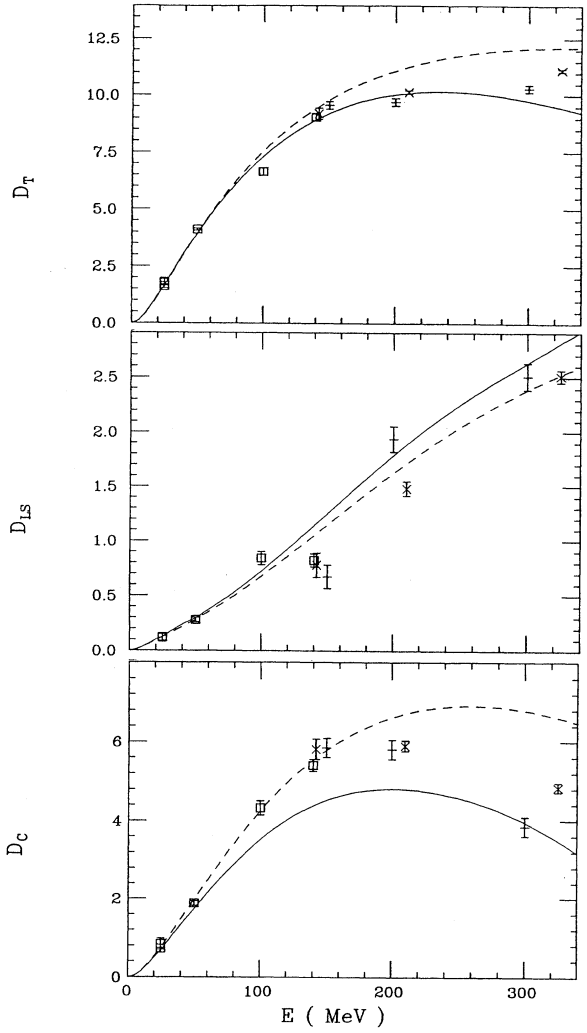

FIG. 9. Central, *LS*, and tensor phase combinations of the *D* waves. Curves represent potential model predictions (solid curve, full Bonn; dashed curve, Paris); the symbols stand for the fixed-energy PSA's of Ref. [37] (bars), Ref. [40] (crosses), and this analysis (open squares).

experimental zero crossing lies exactly in between the predictions of the Bonn and Paris models, clearly illustrating that A_{zz} is just as well fitted by the models as by our final solution. What is hence needed are measurements which break the correlation between ε_1 and $^1P_1$.

Fortunately, we have two such measurements: A_{yy} and $\Delta\sigma_L$. A_{zz} and A_{yy} represent complementary data sets in the sense that the signs of the correlation between ε_1 and $^1P_1$ are opposite. Using both data sets thus tends to eliminate a possible bias in the determination of ε_1 which would be caused by the correlation to a potentially wrong value of $^1P_1$.

The other measurement is the new $\Delta\sigma_L$ datum [$(-26.5\pm1.2\pm1.6)$ mb]. It is much more sensitive to ε_1 than to $^1P_1$. It is significantly more positive than the predictions of all potential models [-29.9 mb (Bonn), -33.8 mb (Paris), -32.2 mb (Nijmegen)] or of old PSA's, which do not contain the new higher-order spin data (-42.1 mb [37], -28.9 mb (Saclay S80 [38])). In an attempt to estimate the ε_1 values consistent with $\Delta\sigma_L$, we fixed $^1P_1$ to a reasonable average value ($-10.0°$). Agreement with $\Delta\sigma_L$ then required the following ε_1 values at 50 MeV: 2.5° (Bonn), 3.0° (Paris), and 3.6° (Nijmegen). Here we have used a simple energy dependence for ε_1. The large value for the Nijmegen model is due to the initial combination $\varepsilon_1/^1P_1 = 2.3°/-8.6°$.

Comparison with other recent PSA's shows that the high ε_1 result of our analysis is not singular. A preliminary analysis by Bugg [85], including the A_{zz} data but not the Karlsruhe A_{yy} and cross-section data, required $\varepsilon_1 \sim 4°$ around 50 MeV. There is a recent analysis by the Nijmegen group [86], which, however, does not include the Bonn $K_y^{y'}$ data, the Karlsruhe A_{yy}, nor the Uppsala cross sections. Their single energy result at 50 MeV ($\varepsilon_1 = 2.37\pm0.48$) is lower than our value, but still consistent within errors. For energies ≥ 100 MeV, their ε_1 values are significantly lower than ours and those of the analysis of Bugg and Bryan [40]. The latter analysis independently supports the high ε_1 trend in a clear fashion at energies above 200 MeV. It includes new, precise higher-order polarization data and results in unique solutions with small uncertainties (see Figs. 5 and 6). The values of ε_1 from this analysis above 200 MeV are considerably higher than the full Bonn prediction, while they are close to the Nijmegen and Paris predictions.

The discrepancy between the new value for ε_1 and theory is largest with respect to the one-boson-exchange (OBE) approximation Bonn *A* [3] (see Fig. 5), which is characterized by a weak tensor force. This relativistic momentum-space potential is able to accommodate both the binding energy of the triton [3] and the polarization transfer coefficient $K_y^{y'}$ in elastic *p-d* scattering [10] without need for three-body forces. The observed disagreement with calculations based on the full Bonn or Paris potential was blamed on the stronger tensor force of the latter models (for the triton binding, see the discussion in the Introduction). Reference [10] found good agreement between the polarization transfer coefficient $K_y^{y'}$ in elastic *p-d* scattering at 22.7 MeV and a continuum three-nucleon calculation based on the Bonn *A* potential. Predictions based on the Bonn *B* or Paris potential do not fit the data. The crucial point, however, is the complete understanding of other processes which may contribute to $K_y^{y'}$. In fact, these studies were originally motivated by a search for processes such as three-body force and/or off-shell effects. At present, there exist no quantitative estimates on the relative contribution of these effects for three-nucleon continuum observables. In addition, the proper treatment of the Coulomb problem for *p-d* is still unsolved. Since the calculation of Ref. [10] neglects both these effects, we believe that a comparison with regard to ε_1 between our analysis and that of Ref. [10] is only meaningful after a detailed study of possible Coulomb and three-body force and/or off-shell contributions. Clearly, dealing with two nucleons only one avoids the additional complexity of the three-nucleon problem.

For the comparison with potential models, one should bear in mind that the models contain free parameters (e.g., for the Bonn potential there are three coupling constants and three form factors), which are essentially fitted to reproduce the deuteron bound-state properties and *NN* scattering. As discussed in Sec. II, the results of the old PSA's practically provided no constraint because of the large uncertainties and the scatter between different PSA's. Thus the isoscalar tensor component was largely undetermined at energies sufficiently above threshold (30 MeV) where it is no longer constrained by the deuteron properties up to about 300 MeV where ε_1 becomes large enough for a sufficiently reliable determination. Under these circumstances it may not be a surprise that more sensitive, precise data yield ε_1 values which are quite different from the present model predictions. The relevant question in fact is whether the models can be adapted to reproduce the new ε_1 values.

Within meson theory the tensor force is largely produced by the exchange of π and ρ mesons. Thus a large ε_1 can be accommodated either by a strong π or a weaker ρ coupling [3]. With respect to π coupling, some evidence has been provided recently [27,28,43] for even weaker coupling ($g_C^2/4\pi = 13.3\pm0.3$, $g_0^2/4\pi = 13.5\pm0.2$). Possible consequences with respect to the deuteron properties have been discussed in detail in Ref. [33]. It appears from this that such a weak π coupling together with the vector-dominance-model [31] value for the tensor/vector ratio of the ρ coupling reproduces the deuteron properties as well as the conventional combination of π/ρ coupling constants. The vector-dominance model [31] invokes a tensor/vector ratio of 3.7, which is only about half of that used for the full Bonn (6.1) or Paris model (6.6). Given this ambiguity, the uncertainties in the π,ρ form factors, and the fact that π and ρ operate at different ranges, it would be very interesting to study the consequences imposed by a real experimental constraint from ε_1 as is provided by the new data.

B. Charge independence breaking

The other important issue we would like to address is the question of possible charge independence breaking (CIB) effects. Significant charge independence breaking has been deduced by the Nijmegen group [39,87,88] from

a PSA of all *np* and *pp* data below 30 MeV. They used a formalism which allowed for CIB by fitting separate coupling constants for $NN\pi^0$ and $NN\pi^{\pm}$. In terms of phase shifts, the observed CIB transformed not only into a splitting of the S waves—as is customary—but also into a large splitting for the P waves. We list in column 1 of Table III the splittings obtained by Ref. [39], after having corrected linearly for the decrease in CIB due to the proper treatment of the magnetic moment interaction [89]. Reference [39] observed the largest effect for the $^3P_0$ wave, with a splitting of almost 20%.

In the meanwhile two groups have reported evidence for charge independence, however, for much reduced values of both the neutral and charged pion coupling constant: the Nijmegen group analyzed *pp* scattering [43] as well as $\bar{p}p \rightarrow \bar{n}n$ [28] to obtain $NN\pi^0$ and $NN\pi^{\pm}$, whereas the VPI Blacksburg group (for a summary of their work, see Ref. [27]) reanalyzed πN scattering.

Motivated by the initial observation [39] of an apparent charge splitting in the S and P waves, we have studied the problem independently by making fits to *np* and *pp* data separately. Column 3 of Table I lists the differences $\Delta = \delta_{pp} - \delta_{np}$ between *np* and *pp* analyses. The errors given are the combined errors of the fits and are, of course, heavily dominated by the uncertainty of the *np* analysis. To our knowledge this is the first time that a PSA based purely on *np* data allowed for a reliable determination of all leading phases (the actual solution is given in column 3 of Table I). We see no evidence for a systematic, large CIB in the P waves, although the large Nijmegen $^3P_0$ splitting is not ruled out.

The above discussion is closely linked to the question of whether there exist other solutions which fit the data equally well. This issue was raised recently in Refs. [90,91]. Reference [90] used a restricted amount of analyzing power data to perform PSA's with the aim of studying possible ambiguities in the P waves, which were already hinted at by Ref. [45]. They find similarly low χ^2 values for various combinations of drastically different P waves, leaving room for a large isospin splitting of the P waves. We list in Table III, column 2, the splittings which were finally used in that study to calculate low-energy *n-d* scattering observes. It was in fact shown [90] that such a splitting would reconcile theory with the experimental data for A_y in elastic *n-d* scattering around 10 MeV [92,93].

We have tested whether our fits represent unique solutions. This is certainly the case at 25 and 50 MeV where we have carefully scanned over a wide range for the leading phases to search for hidden ambiguities. Based on the full analysis of all the data as well as on *pp* or *np* data only, we observed no indication for such ambiguities. To be specific, charge splittings in the P waves corresponding to those recommended by Ref. [90] at 25 and 50 MeV yield χ^2's which are higher by 57 and 97 in comparison to the nominal solutions given in Table I. Obviously, the problem with the analysis of Ref. [90] is that it is based only on a very restricted database (in this case a limited amount of analyzing power data).

VI. CONCLUSIONS

The phase-shift analysis presented is based on the carefully reviewed world $pp+np$ data between 15 and 160 MeV, including the results of five recent measurements of higher-order spin observables in *np* scattering. The improved database allowed for highly stable solutions at 25 and 50 MeV. At 25 MeV a ten-parameter fit based purely on *np* data showed excellent agreement with the corresponding *pp* analysis and provides no indication of anomalous charge independence breaking.

Inclusion of the new higher-order spin data resulted in a much more precise determination of the $^3S_1$-$^3D_1$ tensor mixing parameter ε_1 at 25 and 50 MeV. The analysis presents strong indication for a large isoscalar tensor force at energies above 30 MeV. This is in agreement with recent data and an analysis above 200 MeV, but is in conflict with current potential models. We argue that the models should be updated using the information now available on ε_1. For the first time, ε_1 provides a stringent constraint for modeling the tensor force at energies most relevant for nuclear-matter calculations. This can be expected to clarify the nature of the π and ρ meson contribution to the tensor force in more detail.

ACKNOWLEDGMENTS

The author wishes to thank R. A. Arndt for his help with the analysis code. Discussions with D. V. Bugg, J. Friar, W. Glöckle, K. Holinde, R. Machleidt, I. Slaus, I. Sick, J. J. de Swart, and W. Tornow are gratefully acknowledged.

[1] J. Schwinger, Phys. Rev. **55**, 235 (1939).
[2] H. A. Bethe, Phys. Rev. **57**, 728 (1940).
[3] R. Machleidt, Adv. Nucl. Phys. **19**, 189 (1989).
[4] S. Ishikawa and T. Sasakawa, Phys. Rev. C **36**, 2037 (1987).
[5] R. A. Brandenburg, G. S. Chulik, R. Machleidt, A. Picklesimer, and R. M. Thaler, Phys. Rev. C **37**, 1245 (1988).
[6] R. Machleidt, K. Holinde, and C. Elster, Phys. Rep. **149**, 1 (1987).
[7] R. A. Brandenburg, G. S. Chulik, R. Machleidt, A. Picklesimer, and R. M. Thaler, Phys. Rev. C **38**, 1397 (1988).
[8] M. F. Jiang, R. Machleidt, and T. T. S. Kuio, Phys. Rev. C **41**, 2346 (1990).
[9] H. Witala, W. Gloeckle, and T. Cornelius, Nucl. Phys. **A496**, 446 (1989).
[10] M. Clajus, P. M. Egun, W. Gruebler, P. Hautle, I. Slaus, B. Vuaridel, F. Sperisen, W. Kretschmer, A. Rauscher, W. Schuster, R. Weidmann, M. Haller, M. Bruno, F. Cannata, M. D'Agostino, H. Witala, Th. Cornelius, W. Gloeckle, and P. A. Schmelzbach, Phys. Lett. B **245**, 333 (1990).
[11] H. Arenhoevel, Prog. Theor. Phys. Suppl. **91**, 1 (1987).
[12] I. Sick, *The Three-Body-Force in the 3N System,* Vol. 260 of *Lecture Notes in Physics* (Springer, New York, 1986), p. 42.

[13] T. E. O. Ericson and M. Rosa-Clot, Annu. Rev. Nucl. Part. Sci. **35**, 271 (1985).
[14] R. Machleidt, in *Proceedings of the Twelfth International Conference on Few Body Problems in Physics,* Vancouver, Canada, 1989, edited by H. W. Fearing [Nucl. Phys. **A508**, (1990)].
[15] D. V. Bugg, in *Progress in Particle and Nuclear Physics,* edited by D. H. Wilkinson (Pergamon, Oxford, 1981), Vol. 7, p. 47.
[16] J. Binstock and R. Bryan, Phys. Rev. D **9**, 2528 (1974).
[17] D. V. Bugg, J. Phys. G **6**, 1329 (1980).
[18] D. V. Bugg, Phys. Rev. C **41**, 2708 (1990).
[19] H. P. Stapp, T. J. Ypsilantis, and N. Metropolis, Phys. Rev. **105**, 302 (1957).
[20] J. M. Blatt and L. C. Biedenharn, Phys. Rev. **86**, 399 (1952).
[21] L. Mathelitsch and B. J. Verwest, Phys. Rev. C **29**, 29 (1984).
[22] D. Y. Wong, Phys. Rev. Lett. **2**, 406 (1959).
[23] N. L. Rodning and L. D. Knudson, Phys. Rev. C **41**, 898 (1990).
[24] K. Holinde and R. Machleidt, Nucl. Phys. **A256**, 497 (1976).
[25] M. Lacombe, B. Loiseau, J. M. Richard, R. Vinh Mau, J. Cote, P. Pires, and R. deTourreil, Phys. Rev. C **21**, 861 (1980).
[26] M. M. Nagels, T. A. Rijken, and J. J. de Swart, Phys. Rev. D **17**, 768 (1978).
[27] R. A. Arndt and R. L. Workman, Phys. Rev. C **43**, 2436 (1991).
[28] R. G. E. Timmermans, T. A. Rijken, and J. J. de Swart, Phys. Rev. Lett. **67**, 1074 (1991).
[29] K. Holinde and A. W. Thomas, Phys. Rev. C **42**, R1195 (1990).
[30] R. Koch and E. Pietarinen, Nucl. Phys. **A336**, 331 (1980).
[31] J. J. Sakurai, *Currents and Mesons* (University of Chicago Press, Chicago, 1969).
[32] G. Hoehler and E. Pietarinen, Nucl. Phys. **B95**, 210 (1975).
[33] R. Machleidt and F. Sammarruca, Phys. Rev. Lett. **66**, 564 (1991).
[34] R. Machleidt (private communication).
[35] G. J. Weisel, W. Tornow, C. R. Howell, M. Al Ohali, P. D. Felsher, Z. M. Chen, J. M. Hanly, J. M. Lambert, P. A. Treado, and R. L. Walter, in *Proceedings of the Twelfth International Conference on Few Body Problems in Physics* [14].
[36] M. Schoeberl, H. Kuiper, R. Schmelzer, G. Mertens, and W. Tornow, Nucl. Phys. **A489**, 284 (1988).
[37] R. A. Arndt, J. S. Hyslop, and L. D. Roper, Phys. Rev. D **35**, 128 (1987).
[38] J. Bystricky, C. Lechanoine-Leluc, and F. Lehar, J. Phys. (Paris) **48**, 199 (1987).
[39] V. G. J. Stoks, P. C. van Campen, T. A. Rijken, and J. J. de Swart, Phys. Rev. Lett. **61**, 1702 (1988).
[40] D. V. Bugg and R. A. Bryan, Nucl. Phys. **A540**, 449 (1992).
[41] D. V. Bugg, Annu. Rev. Nucl. Part. Sci. **35**, 295 (1985).
[42] F. Lehar, J. Phys. (Paris) Colloq. **51**, C6-19 (1990).
[43] J. R. Bergervoet, P. C. van Campen, R. A. M. Klomp, J. L. de Kok, T. A. Rijken, V. G. J. Stoks, and J. J. de Swart, Phys. Rev. C **41**, 1435 (1990).
[44] W. Kretschmer, M. Haller, R. Hoepfl, S. List, A. Rauscher, R. Weidmann, M. Clajus, P. M. Egun, W. Gruebler, M. Bittcher, and P. A. Schmelzbach, in Proceedings of the 7th International Conference on Polarization Phenomena In Nuclear Physics, Contributed Papers, 17A, Paris, 1990 (unpublished).
[45] W. Schuster, Habilitationsschrift (Univ. Erlangen, 1989).
[46] J. Smyrski, S. Kystrin, J. Lang, J. Liechti, H. Luescher, T. Maier, R. Mueller, M. Simonius, J. Sromicki, F. Foroughi, and W. Haeberli, Nucl. Phys. **A501**, 319 (1989).
[47] R. A. Arndt, R. H. Hackman, and L. D. Roper, Phys. Rev. C **15**, 1002 (1977).
[48] R. Dubois, Nucl. Phys. **A377**, 554 (1982).
[49] P. H. Bowen, J. P. Scanlon, G. H. Stafford, J. J. Thresher, and P. E. Hodgson, Nucl. Phys. **22**, 640 (1961).
[50] J. P. Scanlon, P. H. Bowen, G. H. Stafford, J. J. Thresher, and A. Langsford, Nucl. Phys. **41**, 401 (1963).
[51] P. W. Lisowski, R. E. Shamu, G. F. Auchampaugh, N. S. P. King, M. S. Moore, G. L. Morgan, and T. S. Singleton, Phys. Rev. Lett. **49**, 255 (1982).
[52] R. A. Arndt, J. Binstock, and R. Bryan, Phys. Rev. D **8**, 1397 (1973).
[53] M. Auman, F. P. Brady, J. A. Jungerman, W. J. Knox, M. R. McGie, and T. C. Montgomery, Phys. Rev. C **5**, 1 (1972).
[54] J. M. Peterson, A. Bratenahl, and J. P. Stoering, Phys. Rev. **120**, 521 (1960).
[55] D. Bubb *et al.*, Can. J. Phys. **52**, 648 (1974).
[56] T. C. Montgomery, B. E. Bonner, F. P. Brady, W. B. Broste, and M. W. McNaughton, Phys. Rev. C **16**, 499 (1977).
[57] G. Fink, P. Doll, T. D. Ford, R. Garrett, W. Heeringa, K. Hofmann, H. O. Klages, and H. Krupp, Nucl. Phys. **A518**, 561 (1990).
[58] P. W. Lisowski, G. F. Auchampaugh, M. S. Moore, G. L. Morgan, and R. E. Shamu, in Symposium on Neutron Cross Sections from 10 to 50 MeV, edited by M. R. Bhat and S. Pearlstein, Report No. BNL-NCS-51245, 1980, Vol. 1, p. 301.
[59] A. Bol, C. Dupont, P. Leleux, P. Lipnik, P. Macq, and A. Ninane, Phys. Rev. C **32**, 308 (1985).
[60] T. Roennqvist, H. Conde, N. Olsson, R. Zorro, J. Blomgren, G. Tibell, O. Jonsson, L. Nilsson, P. U. Renberg, and S. Y. van der Werf, Phys. Rev. C **45**, R496 (1992).
[61] W. Tornow, C. R. Howell, M. L. Roberts, P. D. Felsher, Z. M. Chen, R. L. Walter, G. Mertens, and I. Slaus, Phys. Rev. C **37**, 2326 (1988).
[62] B. R. S. Simpson and F. D. Brooks, Nucl. Phys. **A505**, 361 (1988).
[63] J. Sromicki, D. Holslin, M. D. Barker, P. A. Quin, and W. Haeberli, Phys. Rev. Lett. **57**, 2359 (1986).
[64] C. Brogli-Gysin, J. Campbell, P. Haffter, M. Hammans, R. Henneck, W. Lorenzon, M. A. Pickar, I. Sick, and S. Burzynski, in Proceedings of the 7th International Symposium on Pol. Phenomena in Nuclear Reactions, Contributed Papers, A10, Paris, 1990 (unpublished).
[65] M. Ockenfels, T. Koeble, M. Schwindt, J. Weltz, and W. von Witsch, Nucl. Phys. **A534**, 248 (1991).
[66] M. Ockenfels, F. Meyer, T. Koeble, W. von Witsch, J. Weltz, K. Wingender, and G. Wollmann, Nucl. Phys. **A526**, 109 (1991).
[67] P. Doll *et al.*, in *Proceedings of the Twelfth International Conference on Few Body Problems in Physics* [14].
[68] H. O. Klages, H. Dobiasch, P. Doll, H. Krupp, M. Oexner, P. Plischke, B. Zeitnitz, F. P. Brady, and J. C.

Hiebert, Nucl. Instrum. Methods **219**, 269 (1984).
[69] J. Wilczynski, J. Hansmeier, F. P. Brady, P. Doll, W. Heeringa, J. C. Hiebert, H. O. Klages, and P. Plischke, Nucl. Phys. **A425**, 458 (1984).
[70] R. Aures, W. Heeringa, H. O. Klages, R. Maschuw, F. K. Schmidt, and B. Zeitnitz, Nucl. Instrum. Methods **224**, 347 (1984).
[71] J. J. Malafany, P. J. Bendt, T. R. Roberts, and J. E. Simmons, Phys. Rev. Lett. **17**, 481 (1966).
[72] M. Hammans, C. Brogli-Gysin, S. Burzynski, J. Campbell, P. Haffter, R. Henneck, W. Lorenzon, M. A. Pickar, I. Sick, J. A. Konter, S. Mango, and B. van den Brandt, Phys. Rev. Lett. **66**, 2293 (1991).
[73] R. Henneck, C. Gysin, M. Hammans, J. Jourdan, W. Lorenzon, M. A. Pickar, I. Sick, S. Burzynski, and T. Stammbach, Nucl. Instrum. Methods A **259**, 329 (1987).
[74] M. A. Pickar, S. Burzynski, C. Gysin, M. Hammans, R. Henneck, J. Jourdan, W. Lorenzon, I. Sick, A. Berdoz, and F. Foroughi, Phys. Rev. C **42**, 20 (1990).
[75] B. Van den Brandt, J. A. Konter, S. Mango, and M. Wessler, in *High Energy Spin Physics,* Proceedings of the VIIIth International Symposium, Minneapolis, Minnesota, 1988, edited by K. Heller, AIP Conf. Proc. No. 187 (AIP, New York, 1989), p. 1251.
[76] B. Zihlmann *et al.*, PSI Proposal No. Z-91-02, 1991.
[77] P. Haffter, C. Brogli-Gysin, J. Campbell, D. Fritschi, J. Goetz, M. Hammans, R. Henneck, J. Jourdan, G. Masson, L. M. Qin, S. Robinson, I. Sick, M. Tuccillo, J. A. Konter, S. Mango, and B. van den Brandt, Nucl. Phys. **A548**, 29 (1992).
[78] S. Robinson, R. Henneck, I. Sick, B. van den Brandt, J. A. Konter, and S. Mango, in *Proceedings of the High Energy Spin Physics Conference,* Bonn, 1990, edited by W. Meyer, E. Steffens, and W. Thiel (Springer, New York, 1991), Vol. 2, p. 385.
[79] R. A. Arndt, computer code SAID, 1989.
[80] D. Bandyopadhyay *et al.*, Phys. Rev. C **40**, 2684 (1989).
[81] J. Sowinski, R. C. Byrd, W. W. Jacobs, S. E. Vigdor, C. Whiddon, S. W. Wissink, L. D. Knudson, and P. L. Jolivette, Phys. Lett. B **199**, 341 (1987).
[82] J. Froehlich, L. Streit, H. Zankel, and H. Zingl, J. Phys. G **6**, 841 (1980).
[83] R. A. Arndt, R. H. Hackman, and L. D. Roper, Phys. Rev. C **15**, 1021 (1977).
[84] J. E. Simmons, Rev. Mod. Phys. **39**, 542 (1967).
[85] D. V. Bugg (private communication).
[86] R. A. M. Klomp, V. G. J. Stoks, and J. J. de Swart, Phys. Rev. C **45**, 2023 (1992).
[87] J. R. Bergervoet, P. C. van Campen, T. A. Rijken, and J. J. de Swart, Phys. Rev. Lett. **59**, 2255 (1987).
[88] T. A. Rijken, V. G. J. Stoks, R. A. M. Klomp, J. L. de Kok, and J. J. de Swart, in *Proceedings of the Twelfth International Conference on Few Body Problems in Physics* [14].
[89] V. G. J. Stoks and J. J. de Swart, Nucl. Phys. **A514**, 309 (1990).
[90] H. Witala and W. Gloeckle, Nucl. Phys. **A528**, 48 (1991).
[91] I. Slaus, R. Machleidt, W. Tornow, W. Gloeckle, and W. Witala, Commun. Nucl. Part. Phys. **20**, 85 (1991).
[92] C. R. Howell, W. Tornow, I. Slaus, P. D. Felsher, M. L. Roberts, H. G. Pfuetzner, Anli Li, K. Murphy, R. L. Walter, J. M. Lambert, P. A. Treado, H. Witala, W. Gloeckle, and T. Cornelius, Phys. Rev. Lett. **61**, 1565 (1988).
[93] J. Cub, E. Finckh, H. Friess, C. Fuchs, K. Gebhardt, K. Geissdoerfer, R. Lin, and J. Strate, Few-Body Syst. **6**, 151 (1989).
[94] J. P. Scanlon, G. H. Stafford, J. J. Thresher, P. H. Bowen, and A. Langsford, Nucl. Phys. **41**, 401 (1963).
[95] C. Chih and W. M. Powell, Phys. Rev. **106**, 539 (1957).
[96] A. J. Bersbach, R. E. Mischke, and T. J. Devlin, Phys. Rev. D **13**, 535 (1976).
[97] W. T. Morton, Proc. Phys. Soc. London **91**, 899 (1967).
[98] P. J. Clements and A. Langsford, Phys. Lett. **30B**, 25 (1969).
[99] W. Tornow, P. W. Lisowski, R. C. Byrd, and R. L. Walter, Phys. Rev. Lett. **39**, 915 (1980).
[100] R. Garrett, A. Chisholm, D. Brown, J. C. Duder, and H. N. Buergisser, Nucl. Phys. **A196**, 421 (1972).
[101] W. Benenson, R. L. Walter, and T. H. May, Phys. Rev. Lett. **8**, 66 (1962).
[102] D. T. L. Jones and F. D. Brooks, Nucl. Phys. **A222**, 79 (1974).
[103] G. S. Mutchler and J. E. Simmons, Phys. Rev. C **4**, 67 (1971).
[104] C. L. Morris, T. K. O'Malley, Jr., J. W. Mayr, and S. T. Thornton, Phys. Rev. C **9**, 924 (1974).
[105] D. E. Groce and B. D. Sowerby, Nucl. Phys. **83**, 199 (1966).
[106] A. Langsford, H. Bowen, G. C. Cox, G. B. Huxtable, and R. A. J. Riddle, Nucl. Phys. **74**, 241 (1965).
[107] E. R. Flynn and J. Bendt, Phys. Rev. **128**, 1268 (1962).
[108] R. B. Perkins and J. E. Simmons, Phys. Rev. **130**, 272 (1963).
[109] T. W. Burrows, Phys. Rev. C **7**, 1306 (1973).
[110] T. G. Masterson, Phys. Rev. C **6**, 690 (1972).
[111] L. N. Rothenberg, Phys. Rev. C **1**, 1226 (1970).
[112] F. P. Brady, W. J. Knox, J. A. Jungerman, M. R. McGie, and R. L. Walraven, Phys. Rev. Lett. **25**, 1628 (1970).
[113] M. Drosg and D. M. Drake, Nucl. Instrum. Methods **160**, 143 (1979).
[114] A. Eldred, B. E. Bonner, and T. A. Cahill, Phys. Rev. C **12**, 1717 (1975).
[115] J. L. Romero, M. W McNaughton, F. P. Brady, N. S. P. King, T. S. Subramanian, and J. L. Ullmann, Phys. Rev. C **17**, 468 (1978).
[116] R. Garrett, J. W. Watson, F. P. Brady, D. H. Fitzgerald, J. L. Romero, J. L. Ullmann, and C. Zanelli, Phys. Rev. C **21**, 1149 (1980).
[117] S. W. Johnsen, F. P. Brady, N. S. P. King, M. W. McNaughton, and P. Signell, Phys. Rev. Lett. **38**, 1123 (1977).
[118] D. H. Fitzgerald, F. P. Brady, R. Garrett, S. W. Johnsen, J. L. Romero, T. S. Subramanian, J. L. Ullmann, and J. W. Watson, Phys. Rev. C **21**, 1190 (1980).
[119] N. S. P. King, J. D. Reber, J. L. Romero, D. H. Fitzgerald, J. L. Ullmann, T. S. Subramanian, and F. P. Brady, Phys. Rev. C **21**, 1185 (1980).
[120] D. F. Measday, Phys. Rev. **142**, 584 (1966).
[121] R. Wallace, Phys. Rev. **81**, 493 (1951).
[122] O. Chamberlain and J. W. Easley, Phys. Rev. **94**, 208 (1954).
[123] J. Hadley, E. Kelly, C. Leith, E. Segre, C. Wiegand, and H. York, Phys. Rev. **75**, 351 (1949).
[124] R. G. Stahl and N. F. Ramsey, Phys. Rev. **96**, 1310 (1954).
[125] G. H. Stafford, C. Whitehead, and P. Hillman, Nuovo Cimento **5**, 1589 (1957).
[126] J. J. Thresher, R. G. P. Voss, and R. Wilson, Proc. R. Soc. London **A229**, 492 (1955).

[127] V. Grundies, J. Franz, E. Roessle, and H. Schmitt, Phys. Lett. **158B**, 15 (1985).
[128] A. S. Carroll, P. M. Patel, N. Strax, and D. Miller, Phys. Rev. **134**, B595 (1964).
[129] R. K. Hobbie and D. Miller, Phys. Rev. **120**, 2201 (1960).
[130] W. G. Collins, Jr. and D. G. Miller, Phys. Rev. **134**, B575 (1964).
[131] P. M. Patel, A. Carroll, N. Strax, and D. Miller, Phys. Rev. Lett. **8**, 491 (1962).
[132] V. J. Howard, J. A. Edington, S. S. Das Gupta, I. M. Blair, B. E. Bonner, F. P. Brady, M. W. McNaughton, and N. M. Stewart, Nucl. Phys. **A218**, 140 (1974).
[133] T. C. Randle, D. M. Skyrme, M. Snowden, A. E. Taylor, F. Uridge, and E. Wood, Proc. Phys. Soc. London A **69**, 760 (1956).
[134] G. H. Stafford and C. Whitehead, Proc. Phys. Soc. **79**, 430 (1962).
[135] J. N. Palmieri and Janet P. Wolfe, Phys. Rev. C **3**, 145 (1971).
[136] T. C. Randle, A. E. Taylor, and E. Wood, Proc. R. Soc. London **213**, 392 (1952).